Since January 2020 Elsevier has created a COVID-19 resource centre with free information in English and Mandarin on the novel coronavirus COVID-19. The COVID-19 resource centre is hosted on Elsevier Connect, the company's public news and information website.

Elsevier hereby grants permission to make all its COVID-19-related research that is available on the COVID-19 resource centre - including this research content - immediately available in PubMed Central and other publicly funded repositories, such as the WHO COVID database with rights for unrestricted research re-use and analyses in any form or by any means with acknowledgement of the original source. These permissions are granted for free by Elsevier for as long as the COVID-19 resource centre remains active.

Journal of Fluorine Chemistry 250 (2021) 109865

Contents lists available at ScienceDirect

Journal of Fluorine Chemistry

journal homepage: www.elsevier.com/locate/fluor

Computational studies reveal Fluorine based quinolines to be potent inhibitors for proteins involved in SARS-CoV-2 assembly

Neellohit Sarkar [a,1], Abhimanyu Thakur [b,1], Jigisha Ghadge [b,1], Soumya Lipsa Rath [a,*]

[a] Department of Biotechnology, National Institute of Technology Warangal (NITW), 506004, Telangana, India
[b] Sinhgad College of Pharmacy, Sinhgad Technical Education Society, Vadgaon (Bk), Pune 411041, Maharashtra, India

ARTICLE INFO

Keywords:
Chloroquine
Hydroxychloroquine
Molecular dynamics
Spike-ACE2
TMPRSS2
Virtual screening

ABSTRACT

World is witnessing one of the worst pandemics of this century caused by SARS-CoV-2 virus which has affected millions of individuals. Despite rapid efforts to develop vaccines and drugs for COVID-19, the disease is still not under control. Chloroquine (CQ) and Hydroxychloroquine (HCQ) are two very promising inhibitors which have shown positive effect in combating the disease in preliminary experimental studies, but their use was reduced due to severe side-effects. Here, we performed a theoretical investigation of the same by studying the binding of the molecules with SARS-COV-2 Spike protein, the complex formed by Spike and ACE2 human receptor and a human serine protease TMPRSS2 which aids in cleavage of the Spike protein to initiate the viral activation in the body. Both the molecules had shown very good docking energies in the range of -6kcal/mol. Subsequently, we did a high throughput screening for other potential quinoline candidates which could be used as inhibitors. From the large pool of ligand candidates, we shortlisted the top three ligands (binding energy -8kcal/mol). We tested the stability of the docked complexes by running Molecular Dynamics (MD) simulations where we observed the stability of the quinoline analogues with the Spike-ACE2 and TMPRSS2 nevertheless the quinolines were not stable with the Spike protein alone. Thus, although the inhibitors bond very well with the protein molecules their intrinsic binding affinity depends on the protein dynamics. Moreover, the quinolines were stable when bound to electronegative pockets of Spike-ACE2 or TMPRSS2 but not with Viral Spike protein. We also observed that a Fluoride based compound: 3-[3-(Trifluoromethyl)phenyl]quinoline helps the inhibitor to bind with both Spike-ACE2 and TMPRSS2 with equal probability. The molecular details presented in this study would be very useful for developing quinoline based drugs for COVID-19 treatment.

1. Introduction

In the year 2019, we saw the emergence of a highly contagious disease known as COVID-19. The disease was caused by the novel *betacoronavirus* known as SARS-CoV-2 [1]. The virus is believed to have originated primarily from animal sources which then subsequently spread across the world through human-human contact [2]. This novel form of coronavirus is closely related to SARS-CoV; however, it is much more infectious and mutation prone compared to its predecessors [3]. It has claimed millions of lives across the globe and severely affected several others.

The SARS-CoV-2 is a single-stranded RNA-enveloped virus, encoding 9860 amino acids [4]. The genes express structural and nonstructural proteins. They encode structural proteins such as Spike (S), Envelope (E), Membrane (M) and Nucleocapsid (N) and nonstructural proteins, such as 3-chymotrypsin-like protease, papain-like protease, and RNA-dependent RNA polymerase [5]. SARS-CoV-2 uses the human Angiotensin-converting enzyme 2 (ACE2) receptor for cell entry, in synergy with the host's Transmembrane protease, serine 2 (TMPRSS2) [6].

The Spike is a transmembrane protein with an intracellular domain and an extracellular domain. The trimeric Spike protein can be further divided into S1 and S2 subunits. While, S1 subunit contains the receptor-binding domain (RBD) which interacts with the receptor, the S2 subunit facilitates virus-cell fusion and entry [7,8]. SARS-CoV-2 and SARS-CoV, both require an Angiotensin-converting enzyme 2 (ACE2) receptor for entering the host cells [9]. Transmembrane serine protease 2 (TMPRSS2) is a surface protein expressed in humans. Endothelial cells

* Corresponding author.
E-mail address: slrath@nitw.ac.in (S.L. Rath).
[1] Equal contribution

https://doi.org/10.1016/j.jfluchem.2021.109865
Received 13 July 2021; Received in revised form 6 August 2021; Accepted 7 August 2021
Available online 11 August 2021
0022-1139/© 2021 Elsevier B.V. All rights reserved.

primarily express it throughout the respiratory and digestive tracts. It is believed to be involved in certain pathologies, however, the exact biological function of TMPRSS2 is unknown [6,10,11]. The viral Spike glycoprotein is proteolytically cleaved by TMPRSS2, induces virus-cell membrane fusion at the cell surface and represents one of the essential host factors for initiating SARS-CoV-2 pathogenicity [12,13]. This process is analogous to cell entry and viral activation seen in other coronaviruses, including SARS-CoV, MERS-CoV as well as influenza viruses such as influenza H1N1. The lack of TMPRSS2 in the airways decreases the severity of lung infection by SARS-CoV and MERS-CoV [14,15]. The furin cleavage site is found in SARS-CoV-2 unlike SARS-CoV-1 or any other known sarbecovirus. As mutations at this site decrease viral infectivity it has been established that by acquiring the furin cleavage site the virus has benefitted itself. However, in other mutations in the site of furin cleavage, the infectivity was increased to a great extent [16–20].

Several pharmaceutical companies and research organizations are actively working towards standardizing a treatment strategy for COVID-19. In the later part of 2020, many vaccines have been proposed for COVID-19. However, most of the drugs administered for treatment are based on drug repurposing and those that are used for treatment of flu like diseases [21–23]. HCQ and CQ (CQ) are two well-known drugs that have been used since the early 1900s for the treatment of malaria, rheumatoid arthritis and systemic lupus erythematosus [24,25]. During the 2002 SARS epidemic, various research groups worked on using CQ and HCQ for treatment. Both HCQ and CQ were found to successfully prevent viral replication inside cells [26,27]. It is believed that CQ might prevent the binding of SARS Spike protein and its ACE2 receptor by inhibiting glycosylation [28]. Similarly, HCQ also prevents SARS binding to ACE2 receptors by restricting its interaction with gangliosides [29,30]. Physiologically, HCQ and CQ were found to have increased the pH of the intracellular compartments and degraded the cellular components [26]. Very recently, it has been observed that HCQ was more potent in inhibiting SARS-CoV-2 than SARS-COV and even more effective than CQ [31]. However, both are equally effective in inhibiting virus replication [32]. Several clinical trials, although with small sample size, had found the inhibitory potency of the drug [33]. The preliminary evidence of the drug's effectiveness had even resulted in the worldwide shortage of HCQ and CQ based drugs as a means to prevent COVID-19 [34–36]. Unfortunately, due to lack of sufficient trials and significant and unexpected side-effects, the study has not progressed much [37–41].

Here, we implement an *in-silico* approach combining high throughput docking and computer simulations to propose new HCQ and CQ based analogues. The interactions were mainly studied with Spike, Spike-ACE2 and TMPRSS2 which prove as proteins vital for the establishment of viral contact and entry into the host cell [12,42–46]. We began by docking the CQ and HCQ to the proteins to locate the favorable binding sites [47,48]. Subsequently, we virtually screened a large number of ligands with the quinoline backbone and performed high throughput docking. Based on the docking results, molecular Dynamics (MD) simulations were performed on the best docked complexes. However, the results show a difference in the steadiness of the inhibitors with the proteins. It was found that the Spike-ACE2 complex most favorably binds to quinoline based inhibitors followed by TMPRSS2.

2. Materials and methods

The crystal structures of the proteins were obtained from the Protein Data Bank (PDB IDs: 6W41, 6M17, 2OQ5). The associated protein human antibody CR3302 in 6W41 and B0AT1 complex from 6M17 were manually removed before docking. The spike-ace2 receptor used is in complex with the Receptor Binding Domain (RBD), which comprises binding hotspots of the spike protein to ACE2. Again, since the RBD can fold independently with respect to the rest of the spike protein we considered the complex with the RBD rather than the whole spike protein as reported in earlier papers [49–51].

2.1 Molecular docking

The structures of ligands were downloaded from PubChem database [52]. All docking calculations were performed using Autodock Vina in PyRx software version 0.8 [53]. The protein structures were imported in BIOVIA Discovery Studio visualizer [54] and crystallized water molecules and co-crystallized ligands were removed. The ligand molecules were minimized in the Universal Force Field [55] using the steepest descent algorithm. Only the best docked pose was considered based on binding energies. Each of the docked complexes were further analyzed in the BIOVIA Discovery Studio visualizer for assessment of hydrogen bond and hydrophobic interactions of ligands with protein.

2.2 Virtual screening

Molecular docking studies of HCQ and CQ respectively with the three aforementioned proteins were performed. A library consisting of about 10,000 quinoline analogues was created using the PubChem chemical database. The molecules downloaded were filtered using a Lipinski Rule of Five filter, where approximately 7000 molecules were shortlisted. The protein structures were opened in the BIOVIA Discovery Studio

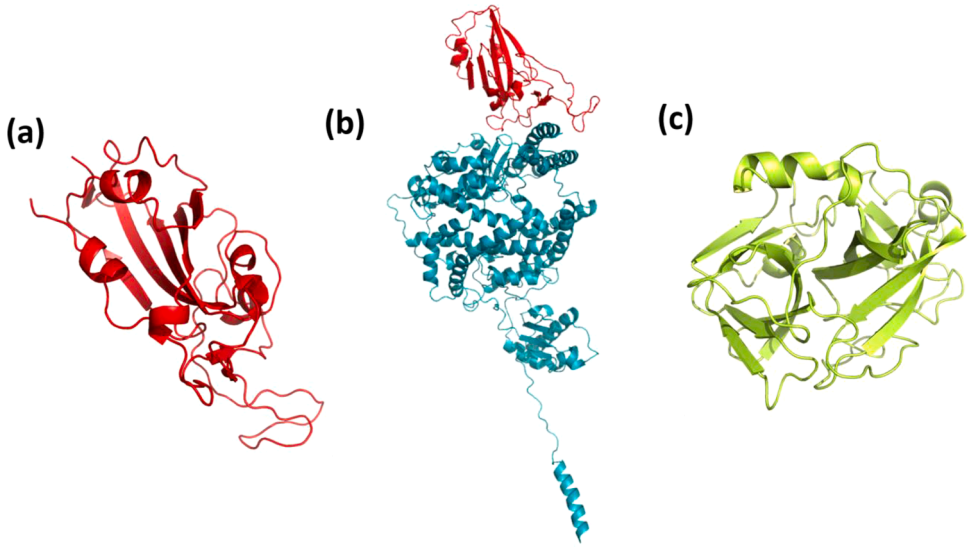

Fig. 1. (a) Structure of Receptor binding domain of Spike protein (shown in red), (b) Spike-ACE2 complex where spike protein is shown in red, ACE2 protein in cyan (c) TMPRSS2 protein.

Table 1
Docking energies of CQ and HCQ with (a) Spike, (b) Spike-ACE2 and (c) TMPRSS2.

	HCQ	CQ
TMPRSS	-6.1	-6
Spike-ACE	-6.1	-5.8
Spike	-6.4	-5.9

visualizer to remove heteroatoms and co-crystallized ligands. The protein structure and the ligands were loaded in PyRx and the ligands were minimized using Universal Force Field to their lowest energy configuration. The binding of these ligands was performed on the active sites of the protein. The interactions of top 10 ligands obtained by High Throughput Screening were studied in the BIOVIA Discovery Studio visualizer.

2.3. MD Simulations

Molecular Dynamics (MD) Simulations were initiated with the top 3 minimum energy configurations by using GROMACS (version 2020.4) MD simulation software package [56]. Charmm36-jul2020 force field was used to get the parameters for protein [57] which was immersed in a water box containing TIP3P water model [58]. The topology and parameters for ligand molecules were generated using the CHARMM General Force Field Server [59]. The docked complexes were placed inside a cubical box with TIP3P water molecules and neutralizing ions. The box dimensions were adjusted in such a way that the box edge was at least 1nm away from the protein-ligand complex. After initial minimization using initially steepest descent and later conjugate gradient algorithms, the system was well-equilibrated in an isochoric-isothermal ensemble at 300 K. This was followed by equilibration at an isothermal-isobaric ensemble. Positional restraints were added to the ligands during the minimization and equilibration. The time step was kept 2 fs. Electrostatic and Van der Waals interaction cut off were kept at 1.2 nm. The long-range electrostatic interactions were treated by using Particle-Mesh Ewald sum and SHAKE was used to constrain all bonds involving hydrogen atoms. After equilibration, the structures were subjected to MD simulation to generate data for analyses.

3. Results and discussion

The crystal structures of Spike protein's receptor binding domain, Spike-ACE2 complex and TMPRSS2 (Fig. 1) were obtained from the protein data bank (PDB IDs: 6W41, 6M17, 2OQ5) [60]. Heteroatoms, such as co-crystallized ligands and water molecules were removed. The associated protein human antibody CR3302 in 6W41 and B0AT1 complex from 6M17 were manually removed before docking. The potential binding sites of the inhibitors were chosen from the previous studies. We began by docking HCQ and CQ to the proteins to ascertain their binding affinities and ligand binding sites. Secondly, we virtually screened 7000 quinoline based small molecule inhibitors to find out the best binding ligands. Finally, we performed Molecular Dynamics (MD) simulations to get more insights on protein-ligand complexes.

3.1. Repurposing HCQ and CQ shows promising results

HCQ (HCQ) and CQ (CQ) have shown potential to inhibit the replication of SARS and SARS-CoV-2 viruses *in vitro* [31,32,61]. To begin with we wanted to study the binding characteristics of HCQ and CQ with the viral Spike protein, the viral Spike and human ACE2 receptor complex and the human protease TMPRSS2 to gain a better understanding of the nature of binding of the drug and proteins.

The large Spike protein has more than thousand residues and is also a transmembrane protein. We selected the receptor binding domain of the Spike protein and docked HCQ and CQ. The active sites for spike protein were obtained from literature review [62,63]. HCQ and CQ, despite having similar chemical structures, it was observed that there were significant differences in their binding energies. The binding energies were -6.4 kcal/mol with HCQ compared to CQ with -5.9 kcal/mol (Table 1). The 0.5 kcal/mol difference in energy can be attributed due to additional interactions of HCQ with the protein including two hydrogen bonding interactions of the ligand with SER469 and ILE472 in the receptor binding domain of Spike protein (Fig. 2). Similarly, we docked the Spike-ACE2 receptor complex with HCQ and CQ. The active sites for docking were taken from literature [64,65]. The complex comprises the RBD of Spike protein and the interacting region of the ACE2 receptor. Spike-ACE2 protein complex was selected because it plays a vital role in the entry of virus, the glycoprotein attaches to the ACE receptor which fuses the virus into the cell membrane [65].

We wanted to check if HCQ and CQ bind to the complex with similar affinities. Upon docking it was observed that the inhibitors docked at the interface of the proteins. Here also the HCQ binding energy (-6.1 kcal/mol) was higher than CQ (-5.8 kcal/mol) (Table 1). Although comparative binding could be observed for both the ligands, presence of unfavorable interactions reduced the overall binding energy (Fig. 2).

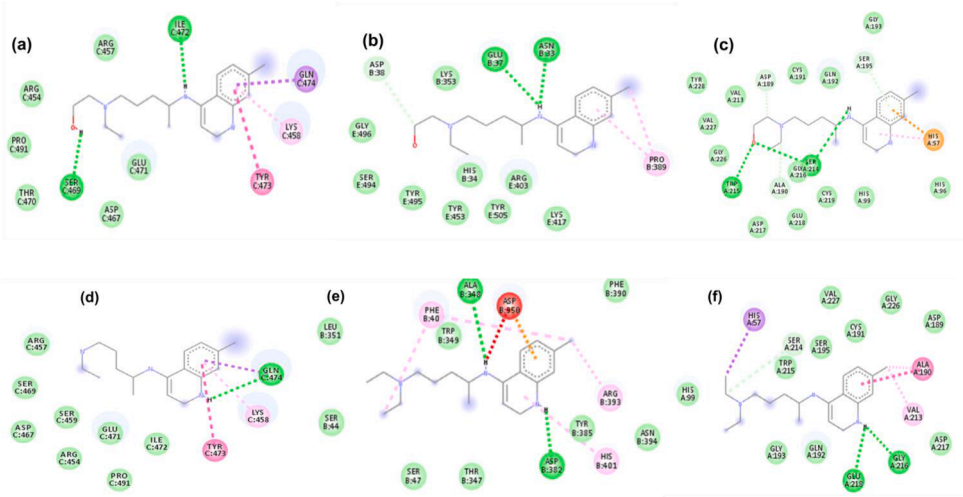

Fig. 2. Binding of HCQ (a-c) and CQ (d-f) with Spike (a, d), Spike-ACE-2 (b, e) and TMPRSS2 (c, f). The figure shows the protein residues interacting with the ligand molecules. The color depicts different interactions; Green for H-bonding, blue for halogen, pink and orange for different interactions involving pi bonds and red for unfavorable interaction.

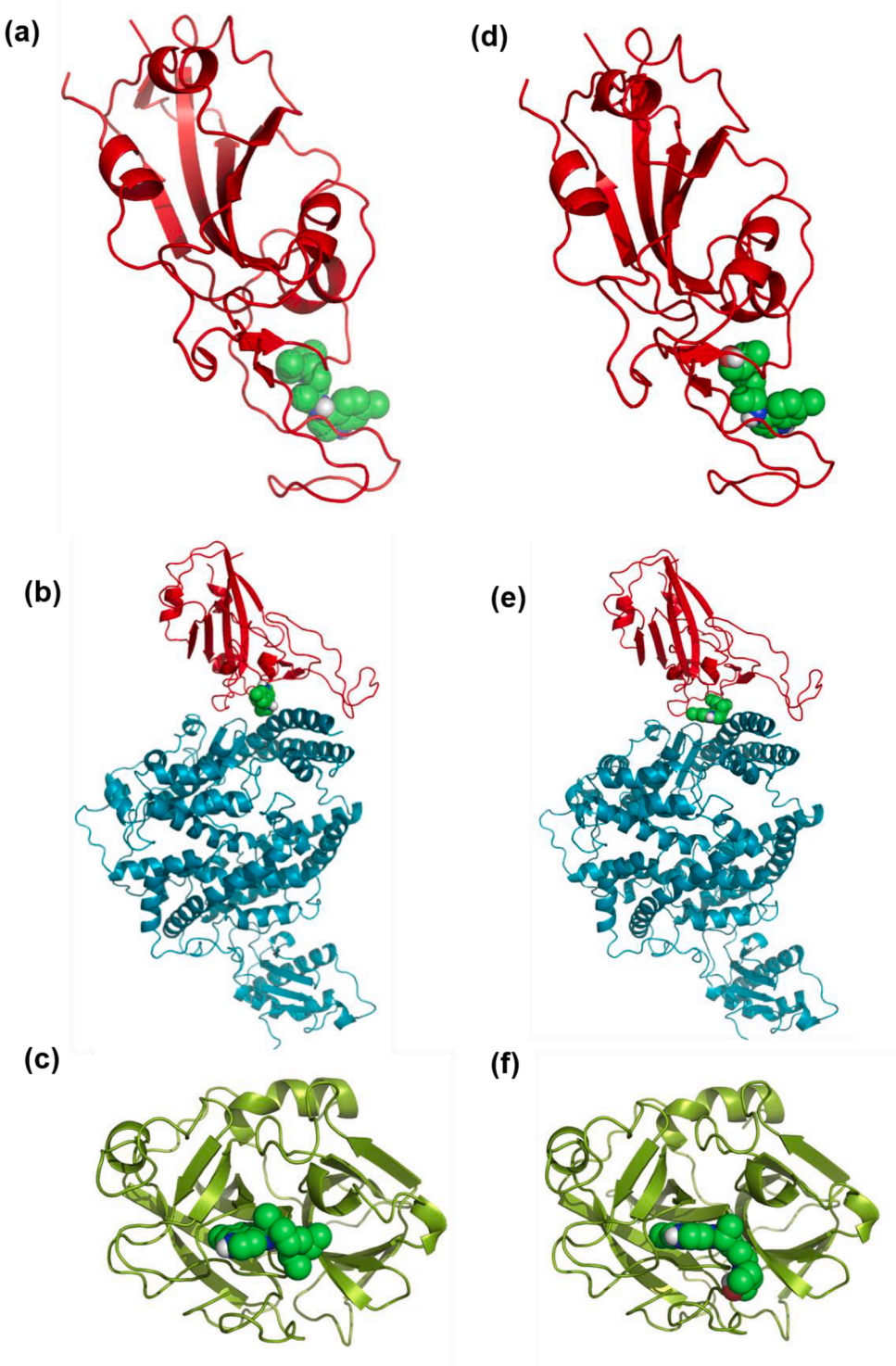

Fig. 3. Binding pocket of CQ (a-c) and HCQ (d-f) bound to Spike (a, d), Spike-ACE-2 (b, e) and TMPRSS2 (c, f). Ligands are shown in green color spheres and the proteins are coded using the same color notation as Fig. 1.

TMPRSS2 is a very significant protein due to its undeniable role in the pathophysiology of SARS-CoV-2 [11,15]. The protease aids the virus in host cell entry and replication. Active sites of the protein were deduced from the earlier literature [44,66]. Surprisingly, the binding energies of HCQ and CQ to TMPRSS2 were found to be very similar (-6.1 kcal/mol and 6 kcal/mol respectively) (Table 1). Nevertheless, we observed more numbers of residues interacting with the ligand in the presence of the polar groups in HCQ (Fig. 2). The binding pockets of all the proteins are shown in Fig. 3 for clarity.

From the above calculations, it is inferred that the HCQ and CQ both could bind well with all the three proteins which have been considered for our study. Furthermore, we could garner a threshold value of the binding energy and the probable binding sites in the proteins. Coadministration of HCQ with antibiotics lead to side effects like QT prolongation, hence administration of HCQ has not been carried out in clinical studies for COVID-19 [67,68]. Thus, we did an extensive search on the alternate quinoline analogues which could prove as alternate candidates for drug designing.

Table 2
Docking energies of top 3 ligands with (a) Spike, (b) Spike-ACE2 and (c) TMPRSS2 obtained by virtual screening.

Protein	Serial No	PubChem CID	Docking Energy (kcal/mol)	Chemical Structures
Spike	1	11482260	-8.8	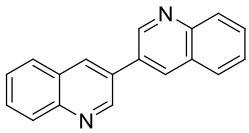
Spike	2	10470033	-8.8	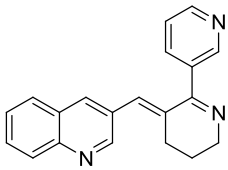
Spike	3	102430872	-8.4	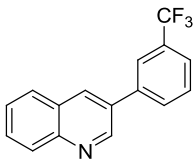
Spike-ACE2	1	10470033	-8.1	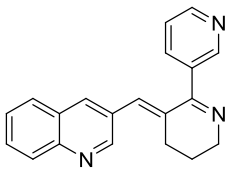
Spike-ACE2	2	102348703	-8.0	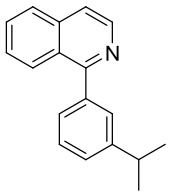
Spike-ACE2	3	102430872	-7.9	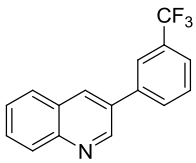
TMPRSS2	1	100955749	-8	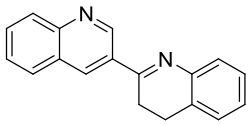
TMPRSS2	2	101186842	-7.6	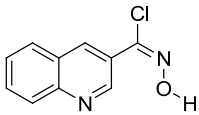
TMPRSS2	3	102430872	-7.6	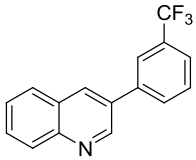

3.2. High throughput screening of HCQ and CQ based inhibitors

For screening quinoline based ligands, an extensive search was performed on PubChem database for the inorganic molecules which followed Lipinski's rule of five, an essential criterion for the druggability of the molecule. 7000 candidates were downloaded from PubChem database to form a quinoline bank. These were docked on all three proteins and top 10 hits from each screening were further subjected to MD Simulations. Consequently, the ligand molecules were minimized using the Universal Force Field and the exhaustiveness of the docking was set to 1 to produce only 1 pose per ligand. One by one all the above proteins were screened for potential drug candidates using the predetermined binding sites. The docking studies were performed to obtain those analogous quinoline molecules whose binding energy surpasses the threshold value obtained for HCQ and CQ. From the previous calculations, the cut off score for ligands were kept to be -6 kcal/mol. A comprehensive list of quinoline based ligands and their docking energies and ADME properties have been provided in Table S2, S3, S4, S5. For each of the proteins, the top three ligands with the maximal docking scores were selected. For all the virtual screening studies, the crystal structure of proteins was the same as before (PDB IDs: 6W41, 6M17, 2OQ5). The top three ligands, along with their structures and their binding scores are given in Table 2.

After obtaining the lead hits from our virtual screening of the quinoline database, we compared the binding of existing protease inhibitors. It was essential to compare our lead compounds after virtual screening to known protease inhibitors to check for similarities in binding interactions of both groups of ligands. Camostat interacted with the protein mainly by conventional hydrogen bonding of which the ligand was a major hydrogen bond donor; a similar pattern was observed in our top ligands which were also bound to the protein by hydrogen donor binding [69]. Likewise, Nafamostat was also bound to the protein by hydrogen donor bonding and unlike Camostat, it exhibits many pi stacking interactions which bear resemblance with the quinoline ligands, apart from the van der Waals interactions. Bromhexine, which is another drug used to inhibit proteases, was bound to the active site of the protein mainly by pi-stacking and van der wails interaction. Our screened ligands are also bound to the protein in a similar fashion, using the pi-pi interactions of the quinoline ring and aromatic amino acid residues present in the active site makes it easier for the ligand to dock easily [70].

It can be very well seen from Table 2 that the quinoline-based ligands bind strongly with Spike, Spike-ACE2 and TMPRSS2 proteins (in the decreasing order of docking energies). Very interestingly, we found one of the molecules 3-[3-(Trifluoromethyl)phenyl]quinoline (ligand 3) binding with a very high affinity with all the three proteins. To elucidate the site of protein-ligand binding we analyzed the residues adjoining the ligands (Fig. 4).

The top 2 ligands which gave the highest docking scores with Spike protein interact with residues ARG393, GLY352, PHE390, PHE40, LEU391, TRP69 during the formation of the complex. It was specifically seen that ARG393 of the Spike protein interacts with all the three ligands. In the first complex, two favorable hydrogen bonds formation could be seen along with a pi-pi stacking interaction which increases its interaction energy; however, a repulsive interaction was also noticed with ASP350. In the second and the third complex, one hydrogen bonding interaction in each was observed. In the case of Spike-ACE2 complex the three ligand-protein interactions that gave the highest docking scores, the ligands interacted with the protein via hydrogen bonding, consistently with the Glu471 residue. Apart from that, common interactions were observed for residues ARG354, SER469, ARG457, GLU471, TYR473, ILE472, LYS458, and GLN474. The regular binding pattern of the ligands to the protein indicates that the quinolines and the analogues bind at the ligand binding pocket in the similar fashion. The three ligands interact with more than fifteen residues of TMPRSS2 in the binding pocket out of which 13 residues are similar. It was especially observed that with ligand 2, salt bridge interactions and as many as 3 hydrogen bonded interactions were there between the protein and ligand. Details of interaction are given in Table S6, S7 and S8.

Since molecular docking is carried out in the absence of any solvent and ions, the role of entropy in the ligand binding has not been taken into consideration. Nevertheless, it is very important to understand the

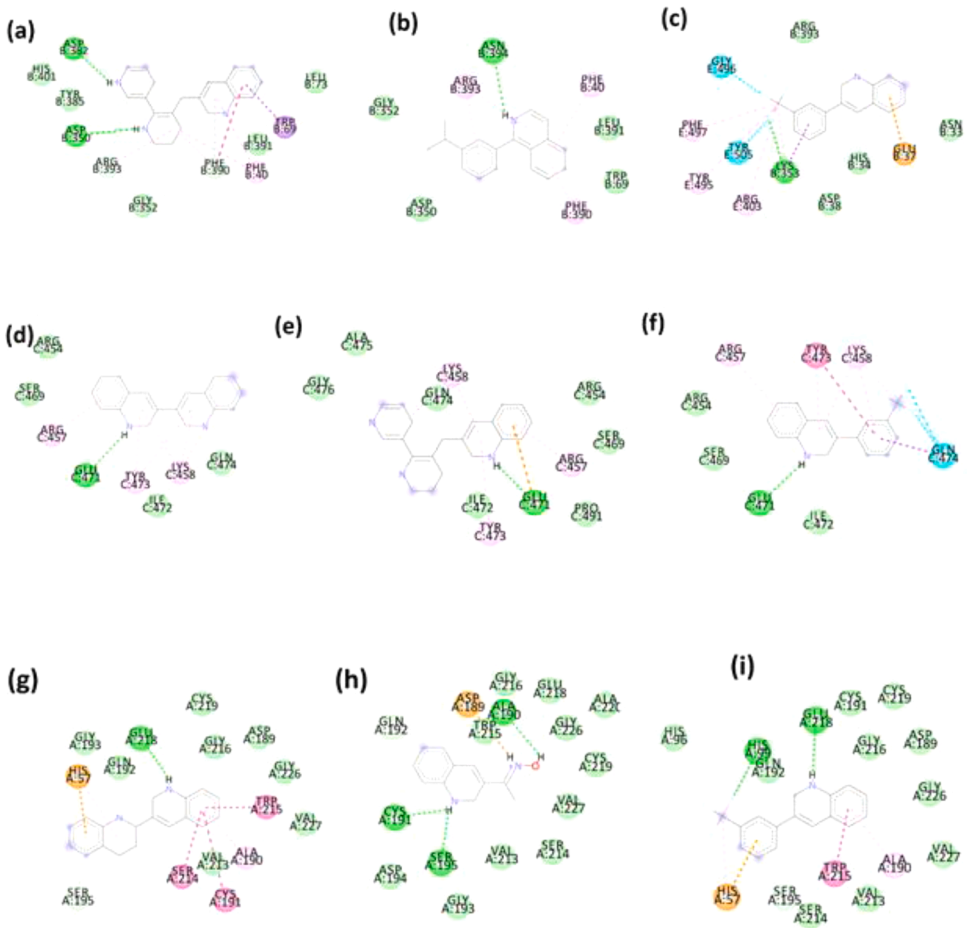

Fig. 4. The top 3 ligands with the highest binding energies with (a-c) Spike protein (d-f) Spike-ACE2 protein complex (g-i) TMPRSS2. The color depicts different interactions; Green for H-bonding, blue for halogen, pink and orange for different interactions involving pi bonds.

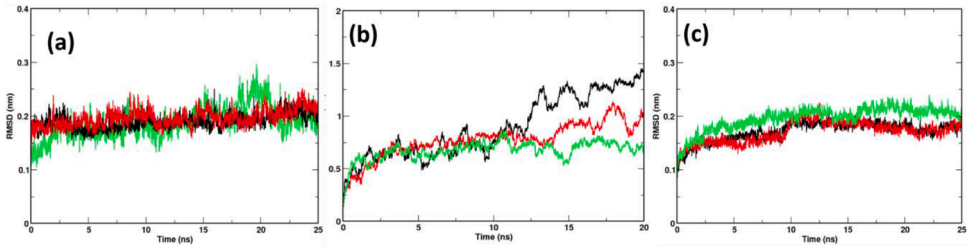

Fig. 5. RMSD of (a) Spike, (b) Spike-ACE2 and (c) TMPRSS2 with the three ligands are shown. Ligands 1, 2 and 3 are colored in black, red and green colors respectively. RMSD of the Spike-ACE2 ligand complex shows the existence of conformational changes.

binding affinity of these ligands in the docked pockets over a period of time under physiological conditions. In order to understand this, we performed MD simulations of the proteins with the docked ligands and studied the changes in interaction over a period of time.

3.3. Protein-ligand binding dynamics

The first three quinoline based inhibitors which showed the highest docking score were subjected to Molecular Dynamics (MD) simulations in order to check the complex stability in nanoseconds time scale and to observe any change in the protein dynamics. After minimization and equilibration, all the protein-ligand complexes were subjected to MD simulations in an NPT ensemble. The ligand parameters were obtained from CGENFF web server. Gromacs 2020.4 and CHARMM36 force field was used for all the simulations (details in materials and methods).

To verify if the systems are stable in an aqueous environment with neutralizing ions, the Root Mean Square Deviation (RMSD) from the initial docked conformation was calculated (Fig. 5). From the RMSDs, it can be seen that Spike ligand complexes had comparable values indicating that all the systems had similar conformation. However, the Spike-ACE2 ligand systems show dramatic RMSD plots. The protein when bound to the third ligand shows the least RMSD value. A major conformational change was observed to have taken place in the Spike-ACE2 ligand 1 complex, Spike-ACE2-ligand 2 also had a higher RMSD value. This indicates that the complex is more stable when bound to the third ligand. RMSF of ACE2 shows similarity of fluctuations in the three complexes (Figure S1). The Spike-ACE2 interactions in wild-type and inhibitor bound complexes. were preserved in all the three complexes (Table S9). In the TMPRSS2 complex, where the ligand binding site is at the central protease pocket of the protein, no remarkable

Table 3
Percentage Occupancy of the ligands in the binding pockets in 20ns MD Simulation.

	Ligand1	Ligand2	Ligand3
Spike	42.35	11.5	28.15
Spike-ACE2	71.7	100	100
TMPRSS2	100	69.7	100

conformational changes in the protein could be deciphered from the RMSD values.

After checking that the proteins are stable, we looked for the ligand occupancy in the binding pockets for all the systems (Table 3). Surprisingly we found that the inhibitors quickly left the binding pocket for all the three spike proteins and had less than 50% occupancy time. To check if this was an artefact, we simulated another docked complex but it also exhibited the same phenomena (data not shown). However, this peculiarity of ligand getting displaced from the binding pocket was not observed in the Spike-ACE2 complexes; in two out of the three systems, the ligand bound very well in the Spike-ACE-2 complex. Similarly, in TMPRSS2 also we observed that two out of three systems displayed stability. Comparison of the ligand binding sites in the initial and final states show that all the three quinoline analogues lost interaction with the Spike protein (data not shown). Thus, despite very high docking scores of ligands with the Spike protein, i.e., >-8 Kcal/mol, the binding affinity of the ligand is greatly affected by the dynamics of the binding site and the solvent environment.

We then checked for the binding of inhibitors to Spike-ACE2 protein. It has been earlier reported that CQ and HCQ bind very well to the Spike-ACE2 complex [71,72]. The docked structures had shown very good binding energies and a consistent hydrogen bond with GLU 471. Thus, we wanted to verify if the structures are stable after simulating it for 20 ns. Out of the three ligands under study, we found that the third ligand bound very well, the second was displaced from the binding pocket but the first ligand had completely left the pocket. Fig. 6 shows that the third ligand has more interactions with the Spike-ACE2 complex when compared to the first two. The binding is facilitated by a strong hydrogen bond with GLU37 and halogen bond formed with GLY496, apart from that LYS353 and TYR505 have hydrophobic interactions with the inhibitor molecule. However, the second inhibitor is displaced from its original position losing in the process many important interactions that were there initially present. LEU73 hydrophobically interacts with the third inhibitor, however, in longer time runs the possibility of displacement of the inhibitor persists. TMPRSS2 is a relatively small protein compared to Spike or ACE2 receptors. When we compared the binding of the ligands only two ligands remained bound to TMPRSS2. Both ligands were observed to have consistent hydrogen bonds with GLN192 during the 20ns of simulation time frame (Fig. 7). Surprisingly, ligand two with salt bridge and large number of hydrogen bonding interactions lost its durability in the binding pocket. But considering an electronegative oxygen atom in the ligand structure, the possibility of repulsive interaction in the binding pocket cannot be ruled out.

One of the major reasons for the greater and effective binding of the fluorinated analogue to the protein receptor is due to the involvement of halogen bonding interactions which are seen in the fluorinated analogues, which involve the Fluorine of the ligand and the amide-carbonyl

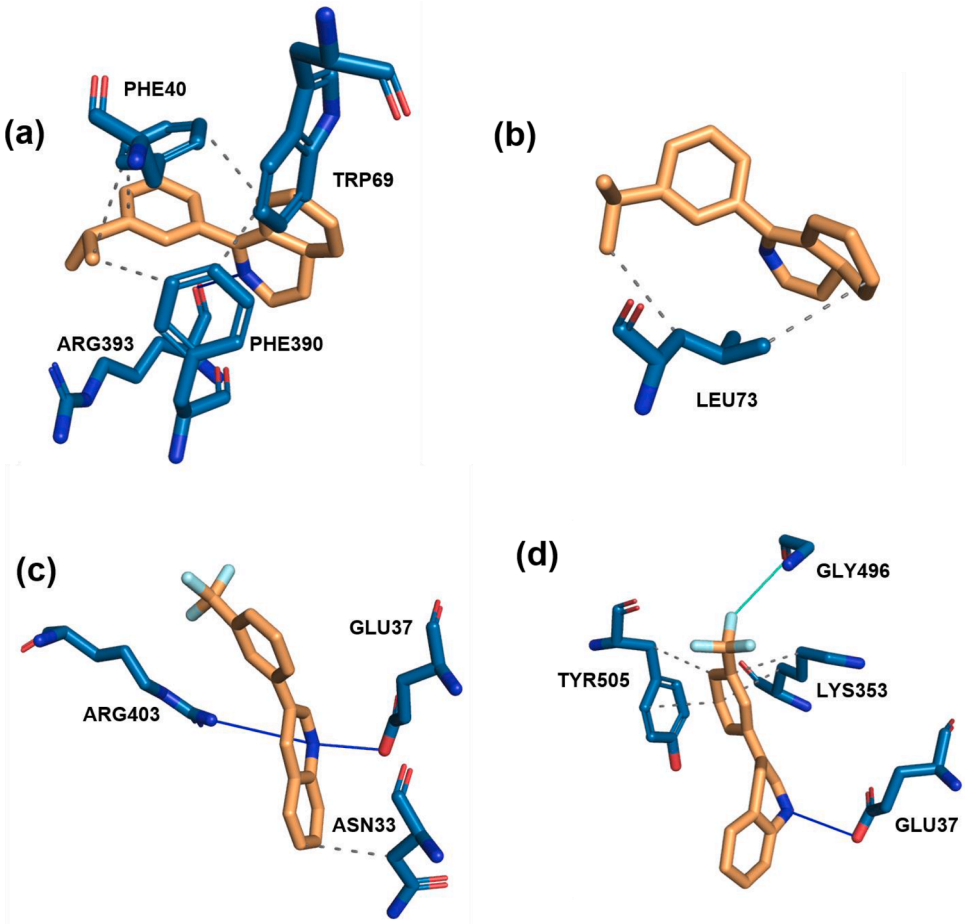

Fig. 6. Starting (a, c) and end (b, d) conformation of SPIKE-ACE2 complex with Ligands 2 (a, b) and 3 (c, d). Protein residues are shown in cyan and ligands are shown in orange color.

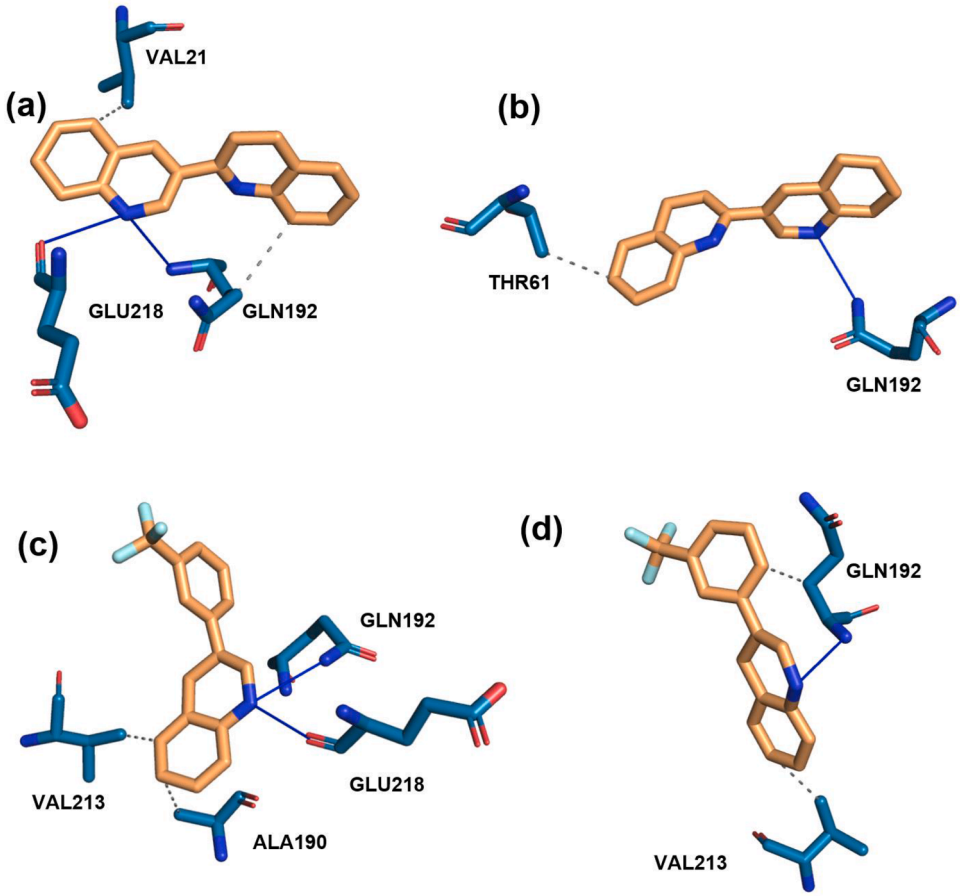

Fig. 7. Starting (a, c) and end (b,d) conformation of TMPRSS2 protein with Ligands 1 (a,b) and 3 (c,d). Protein residues are shown in cyan and ligand is shown in orange color.

group of the protein residues, apart from this there are ring stacking interactions more in the fluorinated analogues as compared to HCQ/CQ. Electronegative GLU37 in Spike-ACE2 helps in the strong binding of quinoline. Similarly, TMPRSS2 inhibitors interacting with GLN192 help its stability. This result matches very well with our initial docked complexes of CQ and HCQ shown in Table 1. Spike-ACE2 interacts with HCQ in the docked complex via a hydrogen bond with GLU37. Similarly, both CQ and HCQ lie very close to GLN192 in docked complexes and could hydrogen bond in the long run. Additionally, one of the inhibitors docked with the proteins was the same, it was found to be quite stable in SPIKE-ACE2 and TMPRSS2 binding pockets.

The vacuum electrostatistics of the docking pockets in the final conformation of Spike-ACE2 and TMPRSS2 show that the inhibitor binding pocket is negatively charged (Fig. 8). Results show that in Spike-ACE2 ligand 2 complex, the ligand is displaced from the docked site due to protein dynamics, the electronegative environment that was seen for the Spike-ACE2 ligand 3 and TMPRSS2 ligand 1 and 3 is different from Spike-ACE2 ligand 2 complex. Therefore, quinolines with electropositive groups would interact with Spike-ACE2 and TMPRSS2 proteins more favorably. The above observations from computational studies would prove very beneficial for fashioning quinoline structure-based drug designing studies for COVID-19.

4. Conclusion

The COVID-19 pandemic has affected crores of individuals all around the world. People are being vaccinated, however, recurrence of disease even after vaccination has been reported. New mutants of SARS-CoV-2 are also observed. In such a scenario, alternative therapeutic strategies by repurposing drugs have also been studied. CQ and HCQ used for treatment of malaria, rheumatoid arthritis and systemic lupus erythematosus were found to successfully prevent viral replication inside cells. However, the drastic side effects, such as QT prolongation, caused by the inhibitors, restricted its application for further treatment of COVID-19. Here, we implement an in-silico approach to propose novel quinoline based inhibitors which could be used as an alternative treatment strategy for COVID-19.

We studied the binding of HCQ and CQ with viral Spike, viral Spike-human ACE2 complex and human TMPRSS2 protease. All of these proteins play a role in initiation and assembly of the virus. Apart from ascertaining the binding site, we also got the threshold value of inhibitor binding energies. Later, we did an extensive search on the alternate quinoline analogues which could prove as promising candidates for drug designing. By our high throughput screening studies carried out for nearly 10000 quinoline based ligands, we were able to identify the best candidates, who also fulfill the ADME characteristics. The docking scores of the inhibitors were found in the range of 8kcal/mol. In order to understand the effect of solvent and protein dynamics in physiological conditions, we performed Molecular Dynamics (MD) simulations of the proteins with the docked ligands and studied the changes in interaction over a period of time.

In MD simulations, we observed that the protein dynamics and effect of solvation does not permit long term stability of ligands with the viral spike protein. None of the ligands remained in the binding pockets with the Spike protein alone. On the contrary, when the quinoline inhibitors bound to Spike-ACE2 protein complex and TMPRSS2 protease, the occupancy of the inhibitors was observed to be for a longer period. It has been observed through many studies that addition of fluorine to ligands

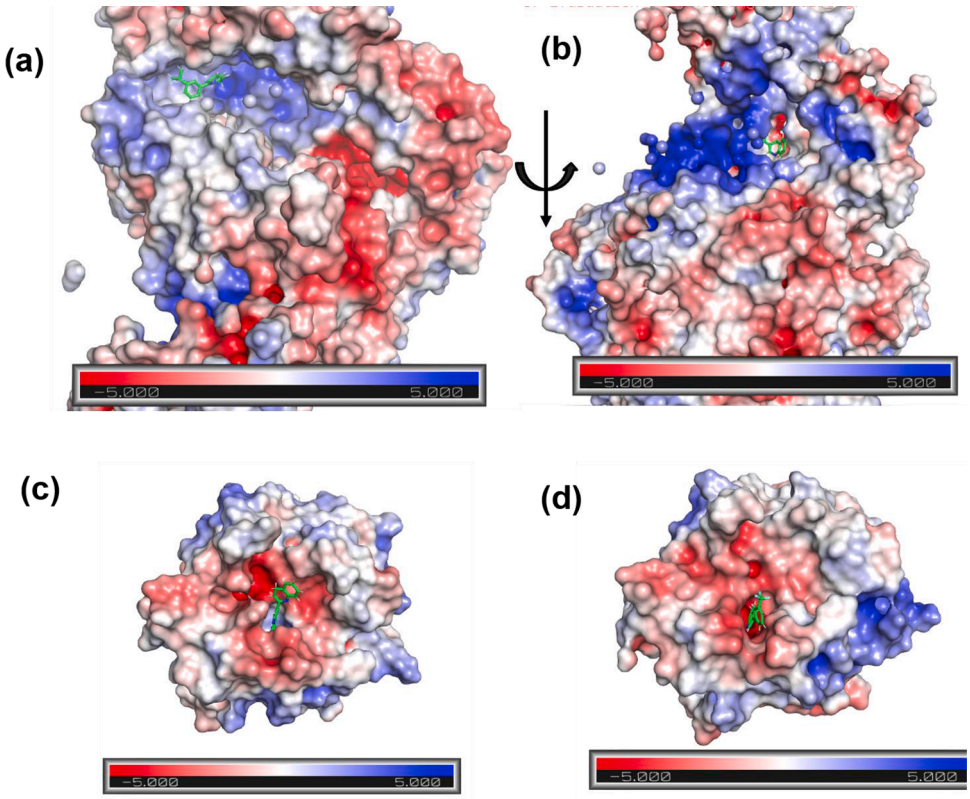

Fig. 8. Electrostatic surface potential calculated by APBS for Spike-ACE protein with ligand 2 (a) and 3 (b) and TMPRSS2 protease with ligand 1 (c) and 3 (d) The ligand molecules are shown as sticks and colored in green. The red and blue color show the electronegative and electropositive surface charges.

has a significant effect not only on the binding of the ligand but also on the physicochemical properties [73]. Firstly, the metabolic stability of the molecules changes significantly, and therefore inclusion of fluorine atoms lends metabolic stability by blocking the labile site [74,75]. Secondly, it is found that fluorine substitution leads to a slight enhancement of binding affinity due to an increased lipophilicity of the molecule and one of the most major effects of fluorine is the way it indirectly influences the acidity/basicity of the ligand. The study by van Niel et al. describes how fluorinated compounds result in drastic improvement in the pharmacokinetic properties of the ligands [76]. In one of the studies by Olsen et al. they showed how the monofluorinated analogue of a thrombin inhibitor binds five times stronger than its non-fluorinated parent compound [77]. The CF3 group containing fluoro- pharmaceuticals is the second largest Fluorine based FDA approved drug and along with mono fluorinated moieties constitute as much as 86% of all FDA approved Fluorine inhibitors. Moreover, fluoroquinolones like ciprofloxacin, norfloxacin, and levofloxacin, are widely used fluoro-pharmaceuticals for treatment. Comparative docking scores are shown in Table S10 [78]. The macromolecular electrostatics shows that the binding pocket is partially negatively charged in nature and would favor the binding of quinoline inhibitors with electropositive groups. From our studies, we found that quinoline based inhibitors prefer binding to TMPRSS2 human protease or viral spike bound to human ACE2 receptors. The inhibitor binding pocket is largely electronegative in nature. The lead compound, 3-[3-(Trifluoromethyl) phenyl]quinoline bound favorably with both Spike-ACE2 complex and TMPRSS2 which could be considered as a candidate for future drug designing studies.

Author contribution

NS, AT and JG designed research; NS, AT, JG and SLR performed research; NS, AT, JG and SLR analyzed data; NS, AT, JG and SLR wrote the paper.

Declaration of Competing Interest

The authors declare that they have no known competing financial interests or personal relationships that could have appeared to influence the work reported in this paper.

Acknowledgements

NS, AT and JG thank the Drug Discovery Hackathon, Government of India for giving a platform to carry out this work. SLR thanks NIT Warangal for research seed grant (P1131) and National Energy Research Scientific Computing Center of the Ernest Orlando Lawrence Berkeley National Laboratory, a DOE Office of Science User Facility supported by the Office of Science of the U.S. Department of Energy under Contract No. DE-AC02-05CH11231 and the Extreme Science and Engineering Discovery Environment (XSEDE). We are grateful to the COVID-19 HPC Consortium for providing resources and helping researchers work for a noble cause.

Supplementary materials

Supplementary material associated with this article can be found, in the online version, at doi:10.1016/j.jfluchem.2021.109865.

References

[1] I. Chakraborty, P. Maity, COVID-19 outbreak: migration, effects on society, global environment and prevention, Sci. Total Environ. 728 (2020), https://doi.org/10.1016/j.scitotenv.2020.138882.
[2] J.S. MacKenzie, D.W. Smith, COVID-19: a novel zoonotic disease caused by a coronavirus from China: what we know and what we don't, Microbiol. Aust. 41 (2020) 45–50, https://doi.org/10.1071/MA20013.

[3] C.C. Lai, T.P. Shih, W.C. Ko, H.J. Tang, P.R. Hsueh, Severe acute respiratory syndrome coronavirus 2 (SARS-CoV-2) and coronavirus disease-2019 (COVID-19): the epidemic and the challenges, Int. J. Antimicrob. Agents. (2020) 55, https://doi.org/10.1016/j.ijantimicag.2020.105924.

[4] S. Seth, J. Batra, S. Srinivasan, COVID-19: targeting proteases in viral invasion and host immune response, Front. Mol. Biosci. 7 (2020), https://doi.org/10.3389/fmolb.2020.00215.

[5] A.A.T. Naqvi, K. Fatima, T. Mohammad, U. Fatima, I.K. Singh, A. Singh, S.M. Atif, G. Hariprasad, G.M. Hasan, M.I. Hassan, Insights into SARS-CoV-2 genome, structure, evolution, pathogenesis and therapies: Structural genomics approach, Biochim. Biophys. Acta - Mol. Basis Dis. 1866 (2020), 165878, https://doi.org/10.1016/j.bbadis.2020.165878.

[6] V. Mollica, A. Rizzo, F. Massari, The pivotal role of TMPRSS2 in coronavirus disease 2019 and prostate cancer, Futur. Oncol. 16 (2020) 2029–2033, https://doi.org/10.2217/fon-2020-0571.

[7] F. Li, Structure, function, and evolution of coronavirus spike proteins, Annu. Rev. Virol. 3 (2016) 237–261, https://doi.org/10.1146/annurev-virology-110615-042301.

[8] Q. Wang, Y. Zhang, L. Wu, S. Niu, C. Song, Z. Zhang, G. Lu, C. Qiao, Y. Hu, K.-Y. Yuen, Structural and functional basis of SARS-CoV-2 entry by using human ACE2, Cell 181 (2020) 894–904, e9.

[9] S. Sharifkashani, M.A. Bafrani, A.S. Khaboushan, M. Pirzadeh, A. Kheirandish, H. Yavarpour_Bali, A. Hessami, A. Saghazadeh, N. Rezaei, Angiotensin-converting enzyme 2 (ACE2) receptor and SARS-CoV-2: potential therapeutic targeting, Eur. J. Pharmacol. 884 (2020), 173455, https://doi.org/10.1016/j.ejphar.2020.173455.

[10] J.D. Strope, C.H.C. PharmD, W.D. Figg, TMPRSS2: potential biomarker for COVID-19 outcomes, J. Clin. Pharmacol. 60 (2020) 801–807, https://doi.org/10.1002/jcph.1641.

[11] M. Thunders, B. Delahunt, Gene of the month: TMPRSS2 (transmembrane serine protease 2), J. Clin. Pathol. 73 (2020) 773–776, https://doi.org/10.1136/jclinpath-2020-206987.

[12] S. Belouzard, J.K. Millet, B.N. Licitra, G.R. Whittaker, Mechanisms of coronavirus cell entry mediated by the viral spike protein, Viruses 4 (2012) 1011–1033, https://doi.org/10.3390/v4061011.

[13] M. Gioia, C. Ciaccio, P. Calligari, G. De Simone, D. Sbardella, G. Tundo, G. F. Fasciglione, A. Di Masi, D. Di Pierro, A. Bocedi, P. Ascenzi, M. Coletta, Role of proteolytic enzymes in the COVID-19 infection and promising therapeutic approaches, Biochem. Pharmacol. (2020) 182, https://doi.org/10.1016/j.bcp.2020.114225.

[14] S. Roychoudhury, A. Das, P. Sengupta, S. Dutta, S. Roychoudhury, A.P. Choudhury, A.B. Fuzayel Ahmed, S. Bhattacharjee, P. Slama, Viral pandemics of the last four decades: pathophysiology, health impacts and perspectives, Int. J. Environ. Res. Public Health. 17 (2020) 1–39, https://doi.org/10.3390/ijerph17249411.

[15] N. Iwata-Yoshikawa, T. Okamura, Y. Shimizu, H. Hasegawa, M. Takeda, N. Nagata, TMPRSS2 Contributes to virus spread and immunopathology in the airways of murine models after coronavirus infection, J. Virol. (2019) 93, https://doi.org/10.1128/jvi.01815-18.

[16] M.O. Pohl, I. Busnadiego, V. Kufner, I. Glas, U. Karakus, S. Schmutz, M. Zaheri, I. Abela, A. Trkola, M. Huber, S. Stertz, B.G. Hale, SARS-CoV-2 variants reveal features critical for replication in primary human cells, PLOS Biol. 19 (2021), e3001006, https://doi.org/10.1371/journal.pbio.3001006.

[17] M. Hoffmann, H. Kleine-Weber, S. Pöhlmann, A multibasic cleavage site in the spike protein of SARS-CoV-2 is essential for infection of human lung cells, Mol. Cell. 78 (2020) 779–784, https://doi.org/10.1016/j.molcel.2020.04.022, e5.

[18] A.C. Walls, Y.-J. Park, M.A. Tortorici, A. Wall, A.T. McGuire, D. Veesler, Structure, function, and antigenicity of the SARS-CoV-2 spike glycoprotein, Cell 181 (2020) 281–292, e6.

[19] J. Shang, Y. Wan, C. Luo, G. Ye, Q. Geng, A. Auerbach, F. Li, Cell entry mechanisms of SARS-CoV-2, Proc. Natl. Acad. Sci. U. S. A. 117 (2020) 11727–11734, https://doi.org/10.1073/pnas.2003138117.

[20] A.K. Padhi, T. Tripathi, Can SARS-CoV-2 accumulate mutations in the S-protein to increase pathogenicity? ACS Pharmacol. Transl. Sci. 3 (2020) 1023–1026, https://doi.org/10.1021/acsptsci.0c00113.

[21] C. Wu, Y. Liu, Y. Yang, P. Zhang, W. Zhong, Y. Wang, Q. Wang, Y. Xu, M. Li, X. Li, M. Zheng, L. Chen, H. Li, Analysis of therapeutic targets for SARS-CoV-2 and discovery of potential drugs by computational methods, Acta Pharm. Sin. B. 10 (2020) 766–788, https://doi.org/10.1016/j.apsb.2020.02.008.

[22] B.N. Rome, J. Avorn, Drug evaluation during the Covid-19 pandemic, N. Engl. J. Med. 382 (2020) 2282–2284, https://doi.org/10.1056/NEJMp2009457.

[23] M. Bilbul, P. Paparone, A.M. Kim, S. Mutalik, C.L. Ernst, Psychopharmacology of COVID-19, Psychosomatics 61 (2020) 411–427, https://doi.org/10.1016/j.psym.2020.05.006.

[24] Z.N. Lei, Z.X. Wu, S. Dong, D.H. Yang, L. Zhang, Z. Ke, C. Zou, Z.S. Chen, CQ and HCQ in the treatment of malaria and repurposing in treating COVID-19, Pharmacol. Ther. (2020) 216, https://doi.org/10.1016/j.pharmthera.2020.107672.

[25] K.D. Rainsford, A.L. Parke, M. Clifford-Rashotte, W.F. Kean, Therapy and pharmacological properties of HCQ and CQ in treatment of systemic lupus erythematosus, rheumatoid arthritis and related diseases, Inflammopharmacology 23 (2015) 231–269, https://doi.org/10.1007/s10787-015-0239-y.

[26] A. Gasmi, M. Peana, S. Noor, R. Lysiuk, A. Menzel, A. Gasmi Benahmed, G. Bjørklund, CQ and HCQ in the treatment of COVID-19: the never-ending story, Appl. Microbiol. Biotechnol. 105 (2021) 1333–1343, https://doi.org/10.1007/s00253-021-11094-4.

[27] M.J. Vincent, E. Bergeron, S. Benjannet, B.R. Erickson, P.E. Rollin, T.G. Ksiazek, N. G. Seidah, S.T. Nichol, CQ is a potent inhibitor of SARS coronavirus infection and spread, Virol. J. 2 (2005), https://doi.org/10.1186/1743-422X-2-69.

[28] T.J. Oscanoa, R. Romero-Ortuno, A. Carvajal, A. Savarino, A pharmacological perspective of CQ in SARS-CoV-2 infection: an old drug for the fight against a new coronavirus? Int. J. Antimicrob. Agents. 56 (2020), 106078 https://doi.org/10.1016/j.ijantimicag.2020.106078.

[29] S. Satarker, T. Ahuja, M. Banerjee, E V.B., S. Dogra, T. Agarwal, M. Nampoothiri, HCQ in COVID-19: potential mechanism of action against SARS-CoV-2, Curr. Pharmacol. Rep. 6 (2020) 203–211, https://doi.org/10.1007/s40495-020-00231-8.

[30] J. Fantini, H. Chahinian, N. Yahi, Leveraging coronavirus binding to gangliosides for innovative vaccine and therapeutic strategies against COVID-19, Biochem. Biophys. Res. Commun. 538 (2021) 132–136, https://doi.org/10.1016/j.bbrc.2020.10.015.

[31] X. Yao, F. Ye, M. Zhang, C. Cui, B. Huang, P. Niu, X. Liu, L. Zhao, E. Dong, C. Song, S. Zhan, R. Lu, H. Li, W. Tan, D. Liu, In vitro antiviral activity and projection of optimized dosing design of HCQ for the treatment of severe acute respiratory syndrome coronavirus 2 (SARS-CoV-2), Clin. Infect. Dis. 71 (2020) 732–739, https://doi.org/10.1093/cid/ciaa237.

[32] A.M. Hashem, B.S. Alghamdi, A.A. Algaissi, F.S. Alshehri, A. Bukhari, M.A. Alfaleh, Z.A. Memish, Therapeutic use of CQ and HCQ in COVID-19 and other viral infections: a narrative review, Travel Med. Infect. Dis. (2020) 35, https://doi.org/10.1016/j.tmaid.2020.101735.

[33] M.S. Khuroo, CQ and HCQ in coronavirus disease 2019 (COVID-19). Facts, fiction and the hype: a critical appraisal, Int. J. Antimicrob. Agents. 56 (2020), https://doi.org/10.1016/j.ijantimicag.2020.106101.

[34] R. Kandimalla, A. John, C. Abburi, J. Vallamkondu, P.H. Reddy, Current status of multiple drug molecules, and vaccines: an update in SARS-CoV-2 therapeutics, Mol. Neurobiol. 57 (2020) 4106–4116, https://doi.org/10.1007/s12035-020-02022-0.

[35] X. Sun, Y. Ni, M. Zhang, Rheumotologitsts' view on the use of HCQ to treat COVID-19, Emerg. Microbes Infect. 9 (2020) 830–832, https://doi.org/10.1080/22221751.2020.1760145.

[36] C. Biguetti, M.T. Marrelli, M. Brotto, Primum non nocere - are CQ and HCQ safe prophylactic/treatment options for SARS-CoV-2 (covid-19)? Rev Saude Publica 54 (2020) 68, https://doi.org/10.11606/s1518-8787.2020054002631.

[37] Y.J. Duan, Q. Liu, S.Q. Zhao, F. Huang, L. Ren, L. Liu, Y.W. Zhou, Trial of CQs in the treatment of COVID-19 and its research progress in forensic toxicology, Fa Yi Xue Za Zhi 36 (2020) 157–163, https://doi.org/10.12116/j.issn.1004-5619.2020.02.002.

[38] L. Alanagreh, F. Alzoughool, M. Atoum, Risk of using HCQ as a treatment of COVID-19, Int. J. Risk Saf. Med. 31 (2020) 111–116, https://doi.org/10.3233/JRS-200024.

[39] U. Paliani, A. Cardona, COVID-19 and HCQ: is the wonder drug failing? Eur J Intern Med 78 (2020) 1–3, https://doi.org/10.1016/j.ejim.2020.06.002.

[40] M.L. Becker, D. Snijders, C.W. van Gemeren, H.J. Kingma, S.F.L. van Lelyveld, T. J. Giezen, QTc Prolongation in COVID-19 patients using CQ, Cardiovasc. Toxicol. 21 (2021) 314–321, https://doi.org/10.1007/s12012-020-09621-2.

[41] L. Alanagreh, F. Alzoughool, M. Atoum, Risk of using HCQ as a treatment of COVID-19, Int. J. Risk Saf. Med. 31 (2020) 111–116, https://doi.org/10.3233/JRS-200024.

[42] M. Yuan, N.C. Wu, X. Zhu, C.C.D. Lee, R.T.Y. So, H. Lv, C.K.P. Mok, I.A. Wilson, A highly conserved cryptic epitope in the receptor binding domains of SARS-CoV-2 and SARS-CoV, Science (80-.) 368 (2020) 630–633, https://doi.org/10.1126/science.abb7269.

[43] R. Yan, Y. Zhang, Y. Li, L. Xia, Y. Guo, Q. Zhou, Structural basis for the recognition of SARS-CoV-2 by full-length human ACE2, Science (80-.) 367 (2020) 1444–1448, https://doi.org/10.1126/science.abb2762.

[44] O.J.P. Kyrieleis, R. Huber, E. Ong, R. Oehler, M. Hunter, E.L. Madison, U. Jacob, Crystal structure of the catalytic domain of DESC1, a new member of the type II transmembrane serine proteinase family, FEBS J. 274 (2007) 2148–2160, https://doi.org/10.1111/j.1742-4658.2007.05756.x.

[45] M. Hoffmann, H. Kleine-Weber, S. Schroeder, N. Krüger, T. Herrler, S. Erichsen, T. S. Schiergens, G. Herrler, N.H. Wu, A. Nitsche, M.A. Müller, C. Drosten, S. Pöhlmann, SARS-CoV-2 cell entry depends on ACE2 and TMPRSS2 and is blocked by a clinically proven protease inhibitor, Cell 181 (2020) 271–280, https://doi.org/10.1016/j.cell.2020.02.052, e8.

[46] A.K. Padhi, T. Tripathi, Targeted design of drug binding sites in the main protease of SARS-CoV-2 reveals potential signatures of adaptation, Biochem. Biophys. Res. Commun. 555 (2021) 147–153, https://doi.org/10.1016/j.bbrc.2021.03.118.

[47] CQ | C18H26ClN3 - PubChem, (n.d.). https://pubchem.ncbi.nlm.nih.gov/compound/CQ (accessed May 15, 2021).

[48] HCQ | C18H26ClN3O - PubChem, (n.d.). https://pubchem.ncbi.nlm.nih.gov/compound/HCQ (accessed May 15, 2021).

[49] A. Spinello, A. Saltalamacchia, A. Magistrato, Is the rigidity of SARS-CoV-2 spike receptor-binding motif the hallmark for its enhanced infectivity? Insights from all-atom simulations, J. Phys. Chem. Lett. 11 (2020) 4785–4790, https://doi.org/10.1021/acs.jpclett.0c01148.

[50] M. Letko, A. Marzi, Functional assessment of cell entry and receptor usage for SARS-CoV-2 and other lineage B betacoronaviruses, Nature.Com (2020) (n.d.) https://www.nature.com/articles/s41564-020-0688-y?report=readeraccessed July 9, 2021.

[51] F. Li, W. Li, M. Farzan, S.C. Harrison, Structural biology: structure of SARS coronavirus spike receptor-binding domain complexed with receptor, Science (80-.) 309 (2005) 1864–1868, https://doi.org/10.1126/science.1116480.

[52] S. Kim, J. Chen, T. Cheng, A. Gindulyte, J. He, S. He, Q. Li, B.A. Shoemaker, P. A. Thiessen, B. Yu, L. Zaslavsky, J. Zhang, E.E. Bolton, PubChem 2019 update: improved access to chemical data, Nucleic Acids Res. 47 (2019) D1102–D1109, https://doi.org/10.1093/nar/gky1033.
[53] G.M. Morris, H. Ruth, W. Lindstrom, M.F. Sanner, R.K. Belew, D.S. Goodsell, A. J. Olson, Software news and updates AutoDock4 and AutoDockTools4: automated docking with selective receptor flexibility, J. Comput. Chem. 30 (2009) 2785–2791, https://doi.org/10.1002/jcc.21256.
[54] Citations and References, (n.d.). https://www.3ds.com/products-services/biovia/resource-center/citations-and-references/(accessed May 15, 2021).
[55] A.K. Rappé, C.J. Casewit, K.S. Colwell, W.A. Goddard, W.M. Skiff, UFF, a full periodic table force field for molecular mechanics and molecular dynamics simulations, J. Am. Chem. Soc. 114 (1992) 10024–10035, https://doi.org/10.1021/ja00051a040.
[56] Lindahl, Abraham, Hess, V.D.S., GROMACS 2021.1 Manual, (2021). https://doi.org/10.5281/ZENODO.4561625.
[57] J. Huang, S. Rauscher, G. Nawrocki, T. Ran, M. Feig, B.L. De Groot, H. Grubmüller, A.D. MacKerell, CHARMM36m: an improved force field for folded and intrinsically disordered proteins, Nat. Methods. 14 (2016) 71–73, https://doi.org/10.1038/nmeth.4067.
[58] P. Mark, L. Nilsson, Structure and dynamics of the TIP3P, SPC, and SPC/E water models at 298 K, J. Phys. Chem. A. 105 (2001) 9954–9960, https://doi.org/10.1021/jp003020w.
[59] K. Vanommeslaeghe, E. Hatcher, C. Acharya, S. Kundu, S. Zhong, J. Shim, E. Darian, O. Guvench, P. Lopes, I. Vorobyov, A.D. Mackerell, CHARMM general force field: a force field for drug-like molecules compatible with the CHARMM all-atom additive biological force fields, J. Comput. Chem. 31 (2010) 671–690, https://doi.org/10.1002/jcc.21367.
[60] H.M. Berman, J. Westbrook, Z. Feng, G. Gilliland, T.N. Bhat, H. Weissig, I. N. Shindyalov, P.E. Bourne, The protein data bank, Nucleic Acids Res. 28 (2000) 235–242, https://doi.org/10.1093/nar/28.1.235.
[61] L. Zou, L. Dai, X. Zhang, Z. Zhang, Z. Zhang, HCQ and CQ: a potential and controversial treatment for COVID-19, Arch. Pharm. Res. 43 (2020) 765–772, https://doi.org/10.1007/s12272-020-01258-7.
[62] A. Basu, A. Sarkar, U. Maulik, Molecular docking study of potential phytochemicals and their effects on the complex of SARS-CoV2 spike protein and human ACE2, Sci. Rep. (2020) 10, https://doi.org/10.1038/s41598-020-74715-4.
[63] P. Bhanu, Comparative molecular docking analysis of the SARS CoV-2 Spike glycoprotein with the human ACE-2 receptors and thrombin, Bioinformation 16 (2020) 532–538, https://doi.org/10.6026/97320630016532.
[64] R. Alexpandi, J.F. De Mesquita, S.K. Pandian, A.V. Ravi, Quinolines-based SARS-CoV-2 3CLpro and RdRp inhibitors and spike-RBD-ACE2 inhibitor for drug-repurposing against COVID-19: an in silico analysis, Front. Microbiol (2020) 11, https://doi.org/10.3389/fmicb.2020.01796.
[65] Y. Zhang, N. Zheng, P. Hao, Y. Cao, Y. Zhong, A molecular docking model of SARS-CoV S1 protein in complex with its receptor, human ACE2, Comput. Biol. Chem. 29 (2005) 254–257, https://doi.org/10.1016/j.compbiolchem.2005.04.008.
[66] J.B. Pierce, V. Simion, B. Icli, D. Pérez-Cremades, H.S. Cheng, M.W. Feinberg, Computational analysis of targeting sars-cov-2, viral entry proteins ace2 and tmprss2, and interferon genes by host micrornas, Genes (Basel) 11 (2020) 1–26, https://doi.org/10.3390/genes11111354.
[67] A.K. Singh, A. Singh, A. Shaikh, R. Singh, A. Misra, CQ and HCQ in the treatment of COVID-19 with or without diabetes: a systematic search and a narrative review with a special reference to India and other developing countries, Diabetes Metab. Syndr. Clin. Res. Rev. 14 (2020) 241–246, https://doi.org/10.1016/j.dsx.2020.03.011.
[68] P. Gautret, J.C. Lagier, P. Parola, V.T. Hoang, L. Meddeb, M. Mailhe, B. Doudier, J. Courjon, V. Giordanengo, V.E. Vieira, H. Tissot Dupont, S. Honoré, P. Colson, E. Chabrière, B. La Scola, J.M. Rolain, P. Brouqui, D. Raoult, HCQ and azithromycin as a treatment of COVID-19: results of an open-label non-randomized clinical trial, Int. J. Antimicrob. Agents. 56 (2020), 105949, https://doi.org/10.1016/j.ijantimicag.2020.105949.
[69] D. Meyer, F. Sielaff, M. Hammami, E. Böttcher-Friebertshäuser, W. Garten, T. Steinmetzer, Identification of the first synthetic inhibitors of the type II transmembrane serine protease TMPRSS2 suitable for inhibition of influenza virus activation, Biochem. J. 452 (2013) 331–343, https://doi.org/10.1042/BJ20130101.
[70] J.H. Shrimp, S.C. Kales, P.E. Sanderson, A. Simeonov, M. Shen, M.D. Hall, An enzymatic TMPRSS2 assay for assessment of clinical candidates and discovery of inhibitors as potential treatment of COVID-19, ACS Pharmacol. Transl. Sci. 3 (2020) 997–1007, https://doi.org/10.1021/acsptsci.0c00106.
[71] R. Badraoui, M. Adnan, F. Bardakci, M.M. Alreshidi, CQ and HCQ interact differently with ACE2 domains reported to bind with the coronavirus spike protein: mediation by ACE2 polymorphism, Molecules 26 (2021), https://doi.org/10.3390/molecules26030673.
[72] I. Celık, A. Onay-Besıkcı, G. Ayhan-Kilcıgıl, Approach to the mechanism of action of HCQ on SARS-CoV-2: a molecular docking study, J. Biomol. Struct. Dyn. (2020) 1–7, https://doi.org/10.1080/07391102.2020.1792993.
[73] H.J. Böhm, D. Banner, S. Bendels, M. Kansy, B. Kuhn, K. Müller, U. Obst-Sander, M. Stahl, Fluorine in medicinal chemistry, ChemBioChem 5 (2004) 637–643, https://doi.org/10.1002/cbic.200301023.
[74] M. Van Heek, C.F. France, D.S. Compton, R.L. McLeod, N.P. Yumibe, K.B. Alton, E. J. Sybertz, H.R. Davis, In vivo metabolism-based discovery of a potent cholesterol absorption inhibitor, SCH58235, in the rat and rhesus monkey through the identification of the active metabolites of SCH48461, J. Pharmacol. Exp. Ther. 283 (1997) 157–163. http://intl-jpet.aspetjournals.org/cgi/content/full/283/1/157. accessed July 4, 2021.
[75] J.W. Clader, The discovery of Ezetimibe: a view from outside the receptor, J. Med. Chem. 47 (2004) 1–9, https://doi.org/10.1021/jm030283g.
[76] D. Kang, S.T. Cheung, A. Wong-Rolle, J. Kim, Enamine N-oxides: synthesis and application to hypoxia-responsive prodrugs and imaging agents, ACS Cent. Sci. 7 (2021) 631–640, https://doi.org/10.1021/acscentsci.0c01586.
[77] J.A. Olsen, D.W. Banner, P. Seiler, U.O. Sander, A. D'Arcy, M. Stihle, K. Müller, F. Diederich, A fluorine scan of thrombin inhibitors to map the fluorophilicity/fluorophobicity of an enzyme active site: evidence for C-F···C=O interactions, Angew. Chemie - Int. Ed. 42 (2003) 2507–2511, https://doi.org/10.1002/anie.200351268.
[78] M Inoue, Y Sumii, N Shibata, Contribution of organofluorine compounds to pharmaceuticals ACS Omega (2020) 10633-10640. doi: 10.1021/acsomega.0c00830.